FINAL PROJECT REPORT

HYDRAULIC MODEL STUDY
POCKET WAVE ABSORBERS

Report UMCEE 99-15

By
Steven J. Wright
And
Donald D. Carpenter

THE UNIVERSITY OF MICHIGAN
DEPARTMENT OF CIVIL AND
ENVIRONMENTAL ENGINEERING
ANN ARBOR, MICHIGAN

December, 1999

For

U.S. Army Corps of Engineers
Detroit District

TABLE OF CONTENTS

LIST OF TABLES

LIST OF FIGURES

1.0 INTRODUCTION

The purpose of this report is to summarize the results of a study completed by the University of Michigan on pocket wave absorbers. The U.S. Army Corps of Engineers (Corps) is using a new technique for wave energy dissipation by installing pocket wave absorbers when updating jetty facilities along the Lake Michigan shoreline. Essentially, a pocket wave absorber is created when a section of a sheet pile wall is set back from the remainder of the jetty wall. Stone is then placed in the pocket to provide a sloping surface, which should dissipate wave energy. This study was conducted to assess the effectiveness of current pocket wave absorbers and to develop design guidelines to assist with future construction.

2.0 BACKGROUND

Many navigational harbors on the Great Lakes use parallel jetty entrances. These jetties, many now in existence for over 100 years, were typically constructed of rock-filled timber cribs. Over time, the timber cribs deteriorated and have been or need to be replaced. The Detroit District of the Corps is responsible for the restoration of many of these structures and has already rehabilitated several sites. The typical rehabilitation approach has been to drive steel sheet pile around the existing structure and to place a concrete cap on top.

After rehabilitation, there was a perception of increased wave heights in the channel. While the rehabilitation restored the structure's effectiveness with respect to wave reflection and overtopping, less wave energy was dissipated. This is apparently because in their deteriorated state, the original timber crib jetties were rough, porous structures that were much more effective at dissipating wave energy than the new sheet pile jetties. To remediate the more energetic wave climate, the Corps removed sections of sheet piling at selected harbors and replaced them with pocket wave absorbers. The effectiveness of these existing wave absorbers has yet to be determined and one of the primary goals of this study is to quantify their effectiveness. The other goal is to develop design guidelines for the construction of any future wave absorbers.

3.0 SCOPE OF WORK

Since the Corps desires both an assessment of existing structures and future design guidelines, there is both a field and a laboratory portion to this study.

The field component is to consist of field measurements of wave heights and energy spectra at four harbors: Pentwater, White Lake, Ontonagon, and Ludington. The first three harbors all have some form of pocket wave absorber in place while the last, Ludington, has an inner harbor with long parallel jetties with sloping stone along their length. Field data will be collected both upstream and downstream of the wave absorbing structures to adequately determine the wave climate between the jetties.

Figure 1 shows the design plans for a pocket wave absorber system at Pentwater, which is typical of the sites with pocket wave absorbers. A photo of the site can be seen in Figure 2.

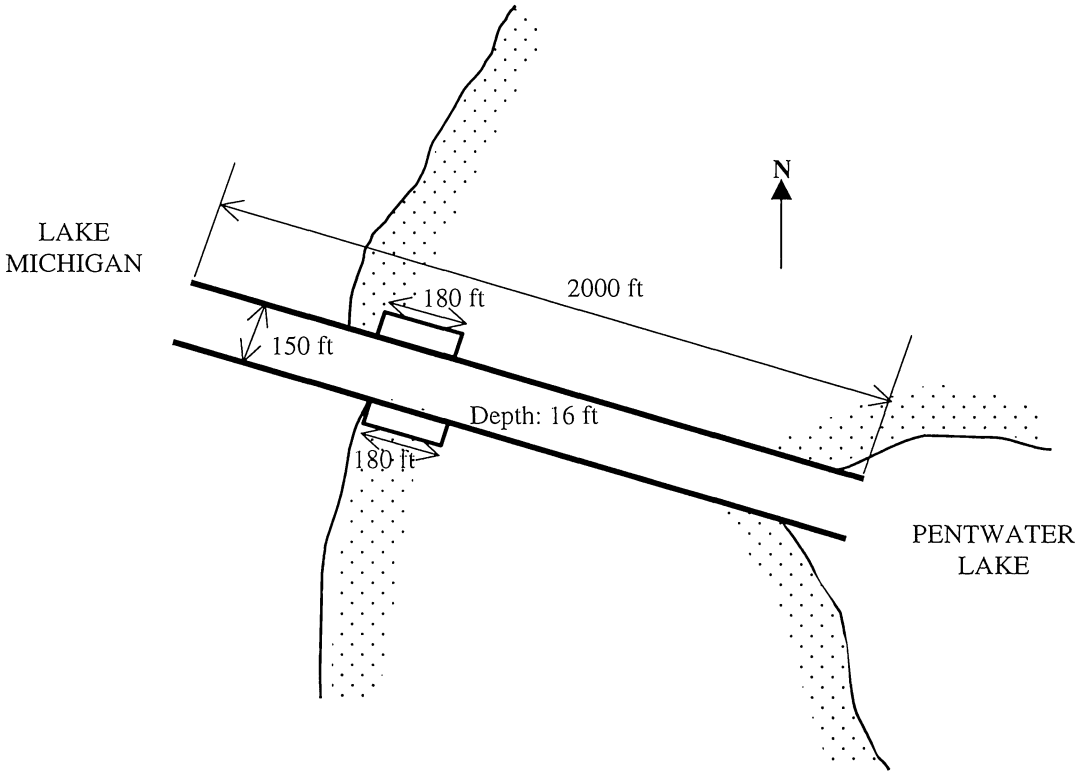

Figure 1: Construction design for the pocket wave absorbers at Pentwater, MI.

Figure 2: South pocket wave absorber at Pentwater, MI.

The lab component consisted of building a physical model of a prototype jetty system and then altering the configuration and location of the pocket wave absorber. This allows isolation of various parameters (such as stone size, stone surface slope, etc.) so that a better understanding of the physical processes surrounding wave absorption by the pockets can be developed.

4.0 ANALYSIS PROCEDURE

4.1 Field Study

The field study portion of this experiment will consist of measuring wave energy in selected harbors. This will be accomplished by placing pressure transducers at two locations between the jetties. The pressure transducers measure pressure fluctuations caused by the surface waves. These fluctuations can then be converted into a wave record using simple wave theory analysis. The attenuation of wave heights in the

direction of wave propagation can then be examined to determine the effectiveness of the wave energy dissipation structure.

Current results are not available due to lack of wave events during the summer months. An energetic wave climate is necessary for evaluating the effectiveness of the pocket wave absorbers and those types of events are rare in the summer months. These events are much more common in the fall and winter, but the waves must also be primarily aligned with the harbor entrance. Recent visits to field sites showed significant wave heights outside of the harbor, but alignment was not appropriate for wave transmission between the jetties. Data will be made available once several appropriate events are monitored.

4.2 Physical Model

A physical model of a typical jetty system was constructed in the University of Michigan Civil and Environmental Engineering Hydraulics laboratory. The physical layout was conceived as a "typical" design from drawings and physical descriptions provided by the U.S. Army Corps of Engineers for Pentwater, White Lake, and Ontonagon harbors. The model was constructed to a nominal linear scale of 1 to 50 (model to prototype). The selection of model scale ratio was based primarily on the available space and the area required for construction of the model. Photos of the laboratory model can be seen in Figures 3 and 4.

The basic model layout (Figure 5) consists of two parallel jetties that are 4 feet apart and 31 feet long with a water depth of 0.32 ft (or approximately four inches). At a 1:50 scale this corresponds to prototype dimensions of 200 feet wide and 1550 feet long with a water depth of 16 ft. Even though water levels can fluctuate significantly in the Great Lakes, 16 ft is a relatively representative water depth. Three wave measurement gauges were then placed permanently at locations corresponding to the channel entrance, mid-channel (near-field with respect to the pocket), and channel exit. The pocket location in the figure is just a sample location as pocket lengths and locations varied during the experiment. The typical pocket geometry can be seen in Figure 6. The variations to

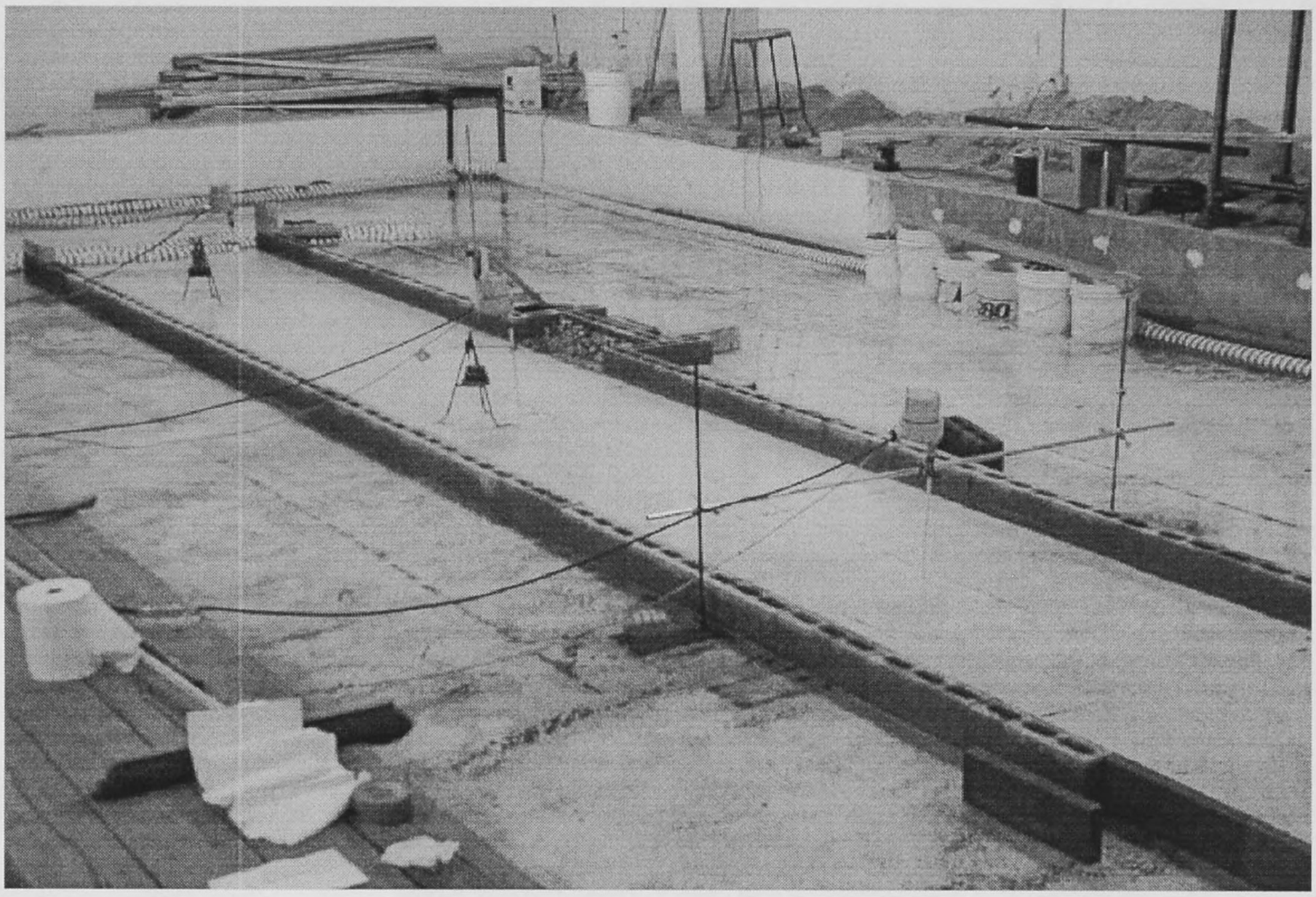

Figure 3: Laboratory model set-up.

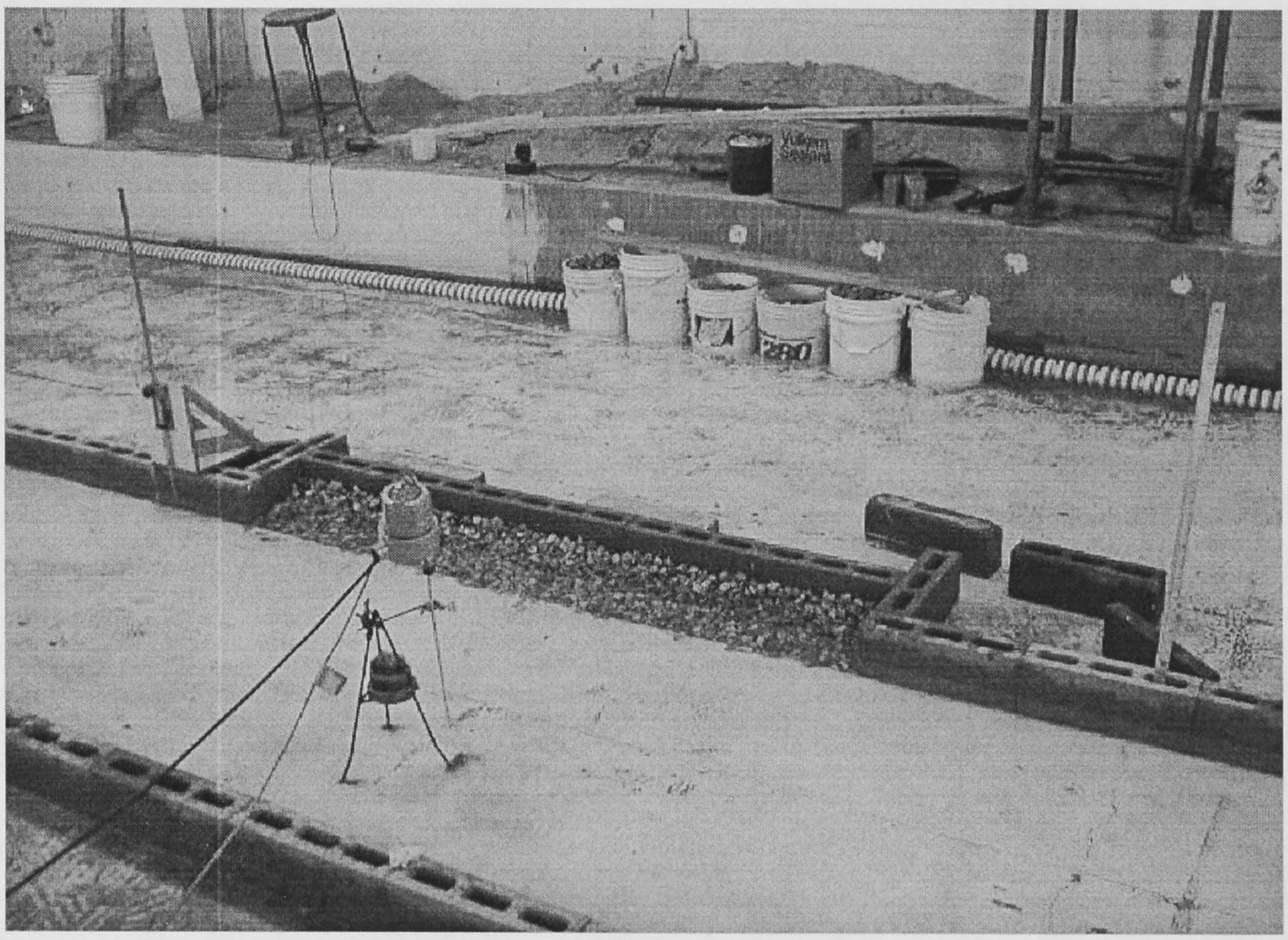

Figure 4: Typical pocket configuration.

the basic model layout represent different test configurations, which were used to isolate and evaluate the following parameters:

- Length of wave absorber
- Slope of stone
- Stone size/void space
- Channel Width
- Location and number of wave absorbers

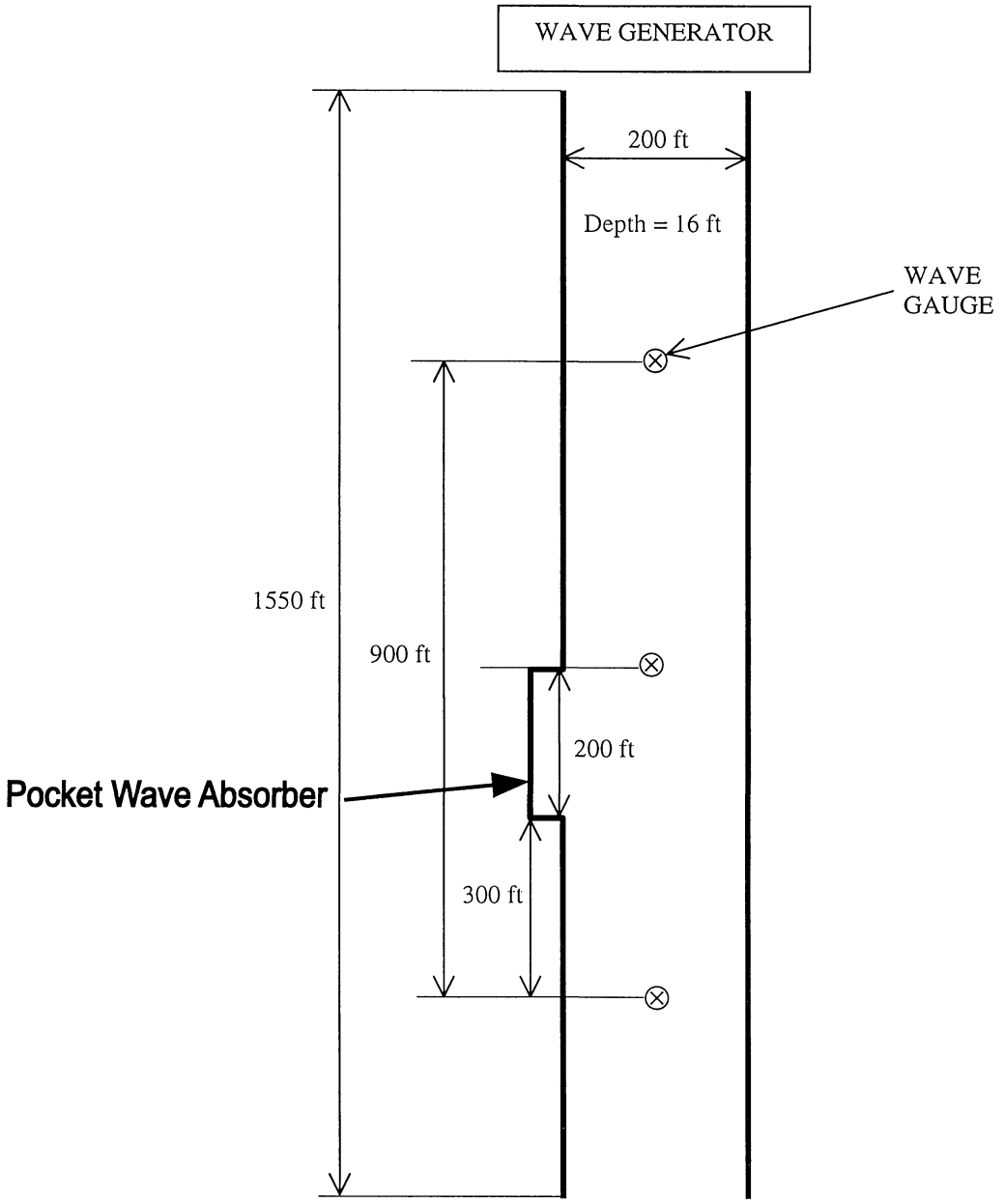

Figure 5: Typical laboratory layout (prototype dimensions for a 1:50 model scale).

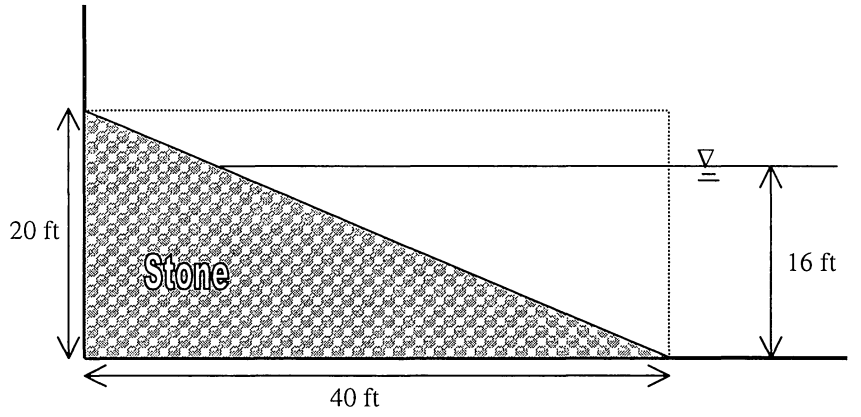

Figure 6: Basic pocket geometry (prototype dimensions for a 1:50 model scale).

The laboratory stone used in the pocket was crushed limestone. To insure uniform stone sizes, the stone was mechanically sieved so that one size of stone will pass one sieve mesh size (example ¾") and be retained on another (example ½"). This sample of stone was then related to a prototypical weight by taking a number of random stones from one sieve size, weighing them, and then scaling up by weight the 1:50 ratio, which scales as $W_{prototype} = W_{model}\,(50)^3$.

The choice of wave conditions studied in the lab was dictated by wave breaking. It was requested that we simulate a "design" wave condition. This was not possible because a design wave would be at or near breaking in 16 ft of water depth. Since breaking waves would seriously limit our ability to draw any conclusions it was decided to set incident waves at just below breaking conditions as determined by the often quoted breaking condition of H/d =0.78. At this wave height severe breaking occurred in the channel. The wave height was then reduced until no significant breaking was observed. This led to prototypical incident waves between 6 to 8 ft and periods between 5.5 to 7 sec. The heights of the incident waves varied during the duration of the experiment due to differences in frequency, water depth, and occasionally channel configuration. While incident waves varied over the duration of the experiment, an effort was made to make the incident wave condition as consistent as possible while evaluating individual parameters.

Wave heights in the model were measured using analog capacitance wave gauges which provide a voltage output proportional to water surface elevation. The gauges send a voltage signal to a data acquisition board, which converts the analog signal to digital output at a specified sampling frequency. The data analysis is performed using LabView software, which converts the voltage signal into a wave height from calibration curves supplied by the user. Finally, the software supplies a continuous record of the water surface, the mean water level, the wave amplitude, and peak frequency for all three gauges.

The mean water level is defined as,

$$\mu = \frac{1}{n}\sum_{i=0}^{n-1} x_i \quad .$$

where x is the water displacement in feet. The wave amplitude is defined as,

$$\sigma = \sqrt{\sigma^2} = \sqrt{\frac{1}{n}\sum_{i=0}^{n-1}(x_i - \mu)^2} \quad ,$$

which is the standard deviation of the wave record. The variance can also be related to the continuous energy spectrum by,

$$\sigma^2 = \int_0^{\infty} E(\omega)\, d\omega \quad ,$$

where $E(\omega)$ is the energy density as a function of the frequency, ω. This relationship associates the wave record to a frequency spectrum. The data analysis software provides the peak frequency, which is associated with the maximum magnitude of $E(\omega)$.

In a true sinusoidal wave the average energy of a wave train is proportional to the average value of the square of the water surface (η^2), which is analogous to the variation of the wave train, σ^2. Therefore, for a sinusoidal wave, the wave amplitude, σ, can be directly related to a maximum wave height ($\sigma = .707\ H_{max}$). Wave amplitude can also be approximately related to typical measurements of wave heights by assuming the Rayleigh distribution is an appropriate description of the wave distribution. Some common wave

height indicators are significant wave height (H_s), root mean square wave height (H_{rms}), and average wave height (H).

$$H_s \approx 4\,\sigma \qquad H_{rms} \approx 2.828\sigma \qquad H \approx 2.506\,\sigma$$

Since wave amplitude is directly related to wave energy and approximately related to wave height, all results are displayed in wave amplitude. The wave amplitude at the first wave gauge is referred to as the incident wave since it is close to the entrance of the jetties. The wave amplitude at the last wave gauge is referred to as the dissipated wave since it has already passed the pocket and been dissipated accordingly. The results from the middle wave gauge are displayed in Appendix A but are not including in any figures since the results are strongly influenced by the proximity to the pocket. When referring to percent dissipation, that is in reference to the incident wave,

$$\%\,dissipated = \frac{(incident\,wave\,amplitude - dissipated\,wave\,amplitude)}{incident\,wave\,amplitude} * 100 \quad .$$

5.0 LABORATORY RESULTS

To evaluate individual variables in the lab, all variables but the one of interest were fixed. This allowed us to isolate the effects of that variable. Also, parameters that were expected to have limited effect were evaluated first. This allowed them to be fixed for a "base" condition when evaluating other parameters.

5.1 Stone Size

Several different stone size cases were tested including four uniform stone sizes, a mix of the largest and smallest uniform stone sizes evaluated, and a well sorted stone. Some of the sizes evaluated are not realistic for real applications, but a broad range was examined to determine effect. To evaluate stone size, the pocket dimensions (40 ft wide by 200 ft long), wave frequency (1 Hz, T = 7.1 sec), and slope (1:2 vertical to horizontal) were all fixed. The results can be seen in Figure 7, which shows the average incident and dissipated wave amplitudes. Overall, for uniform stone sizes, the effect of stone size on

dissipation was negligible. For the four uniform stone sizes, the incoming and dissipated wave amplitudes are all about the same and dissipation rates varied from 57.5 to 63.3 percent. For the case of where the 9 ton stone and 0.25 ton stone were mixed, the dissipation rate is only slightly higher at 64 percent. The final case is for a well-sorted stone with a median weight of 1 ton. In this case the dissipation rate was measurably smaller with a dissipation rate of 50.9 percent. Compared to the other tests, the incident wave was not as large, which makes direct comparison more difficult.

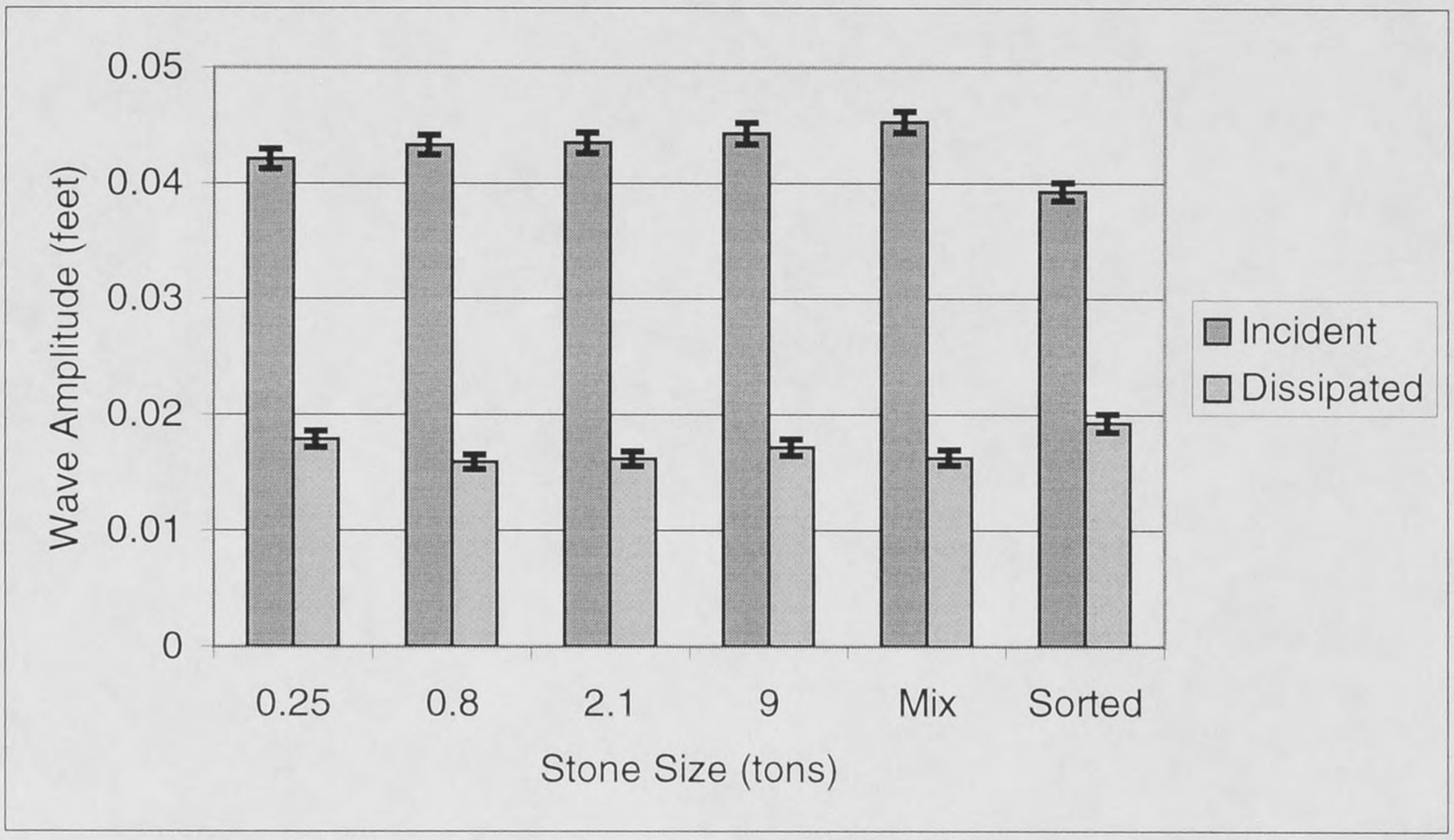

Figure 7: Average incident and dissipated wave amplitudes for variable stone sizes (error bars represent ± 1 standard deviation).

5.2 Slope

Three different slopes of stone where evaluated; 1:1.5, 1:2, and 1:3 (vertical to horizontal), and the test was repeated using two stone sizes (2.1 ton uniform and 1 ton sorted) with different pocket lengths. The 2.1 ton stone was evaluated with a pocket length of 133 ft while the 1 ton sorted stone was evaluated with a pocket length of 400 ft. The wave frequency (1 Hz, T = 7.1 sec) was the same for both. Very different cases were considered to see if the effect of slope was the same for both. The results are displayed in Figure 8, which shows the average incident and dissipated amplitudes. It can be seen that

while the amount of dissipation varied significantly between the two different cases, as would be expected, the variation with slope is limited. The dissipation rates varied from 23.5 to 28.1 percent for the uniform stone size case and from 50.9 to 54.0 for the sorted stone case.

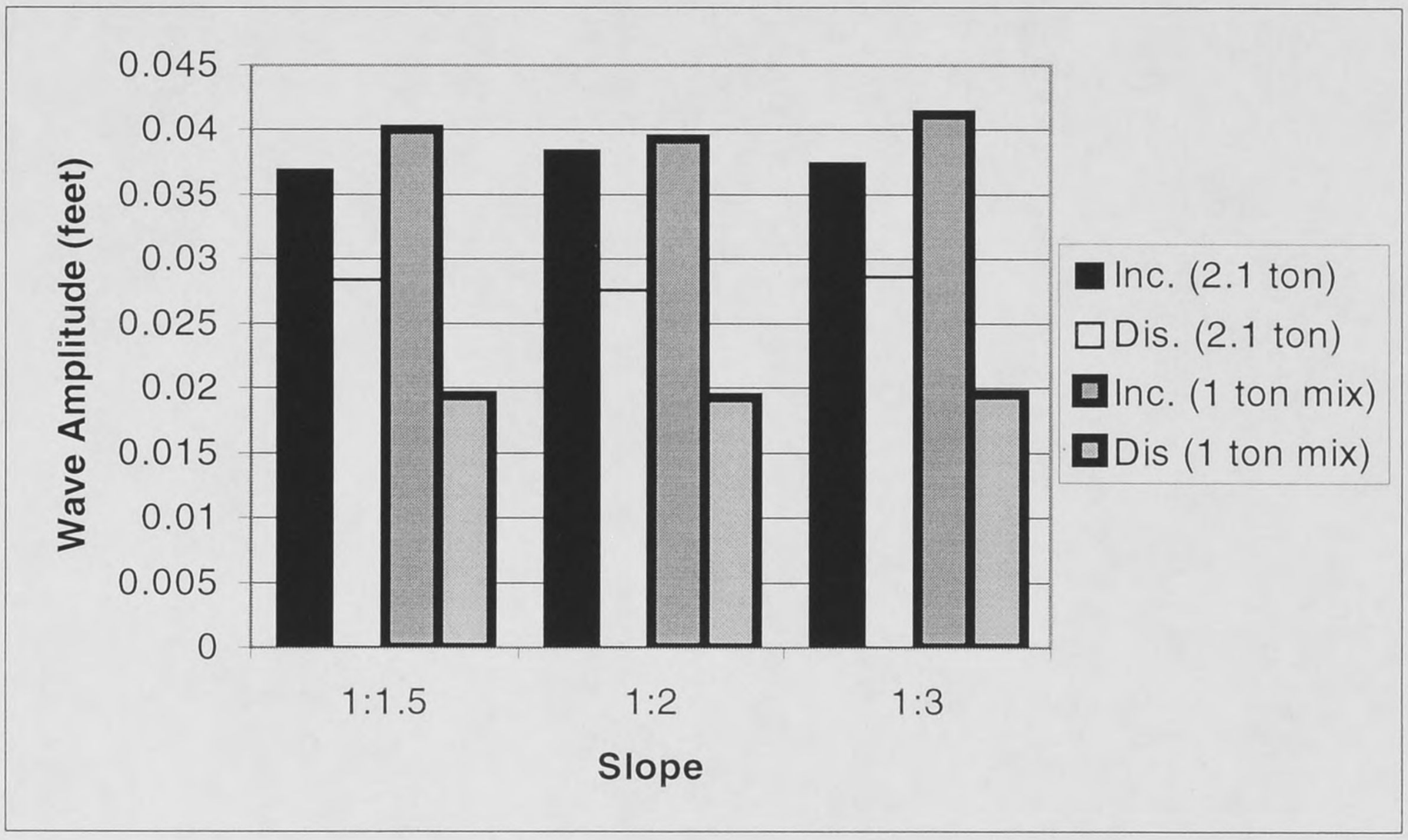

Figure 8: Average incident and dissipated wave amplitudes for variable slopes.

5.3 Pocket Length

From prior tests, a base case was set as a 2 ton stone size, a 1:2 slope, a 1 Hz frequency (T = 7.1 sec), and a pocket depth of 40 ft. Initially, the effect of pocket length was evaluated by varying the prototype pocket length from 133 ft to 400 ft in five even increments. It was found that the dissipation did not increase monotonically with pocket length, but instead varied non-monotonically (Figure 9). This led to the consideration that pocket length, as a singular parameter, was not a determining factor in wave energy dissipation, but rather that the ratio of pocket length to wavelength might be a more significant factor. To further examine the relationship, a second type of testing was devised in which the pocket dimensions were fixed and the frequency of the incident

wave was varied. This allowed us to examine smaller ratios of pocket length to wavelength. For this experiment, the wavelengths were calculated from the frequencies using small amplitude theory.

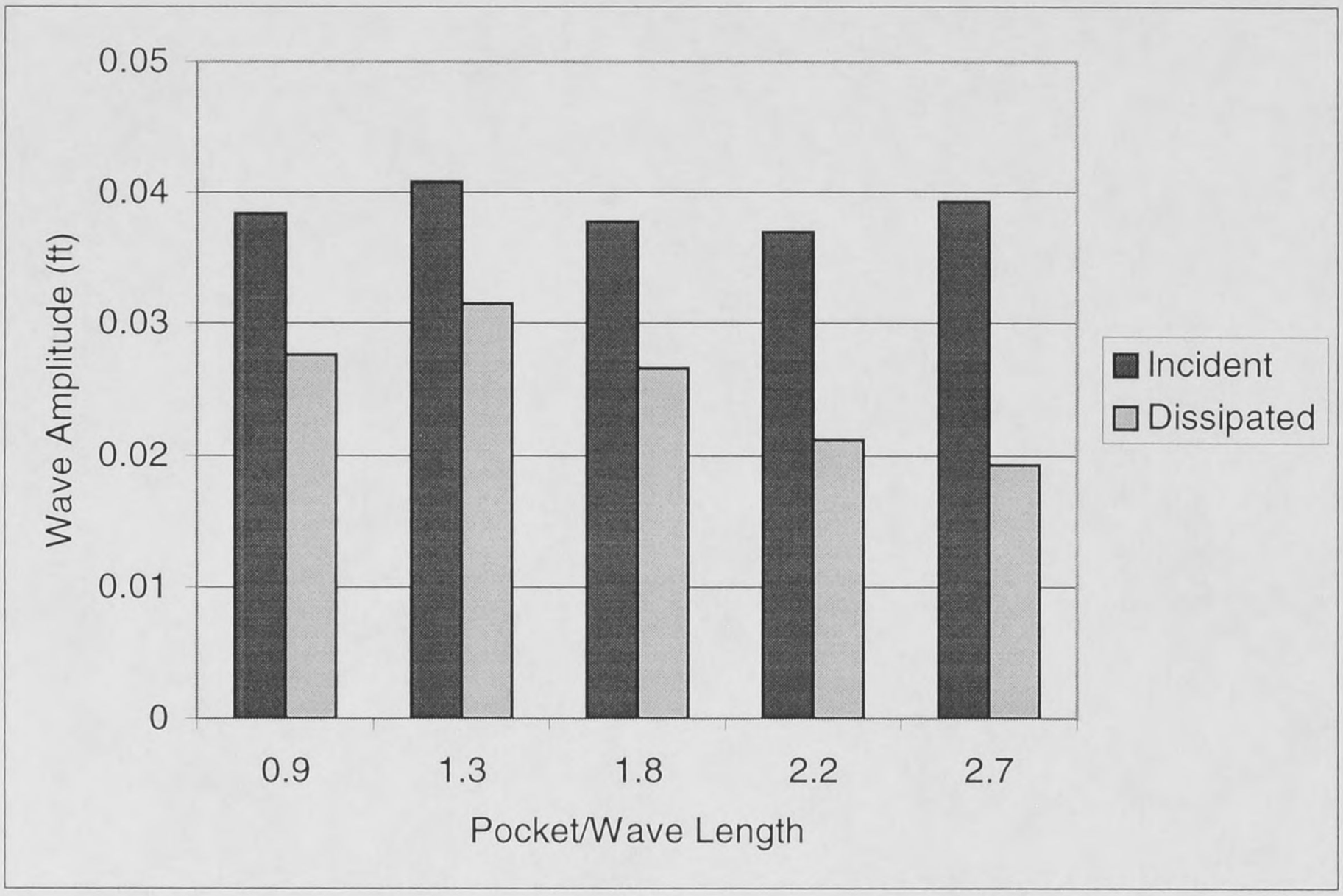

Figure 9: Average incident and dissipated wave amplitudes for fixed frequency test.

Figure 10 shows the results for the four fixed pocket length cases along with the results of the fixed frequency (T = 7.1 sec) variable pocket length cases. Trendlines have been added to connect the individual data points, but that should not be interpreted as the only realization. It can be seen that all cases exhibit significant variation with the maximum dissipation occurring at different intermediate frequency. For the two shorter pockets (95' and 133'), the maximum dissipation occurs at a frequency of 1.1 Hz (T = 6.4 sec), at 1.15 Hz (T = 6.15 sec) for the 167' long pocket, and at 1.2 Hz (T = 5.9 sec) for the 200' long pocket. From these results, it appears that the maximum dissipation is occurring at lower periods as pocket length increases. A more detailed study of the interactions is needed before any significant conclusions can be made. Additionally, it appears as if the dissipation rates drop considerably on either side of the peak.

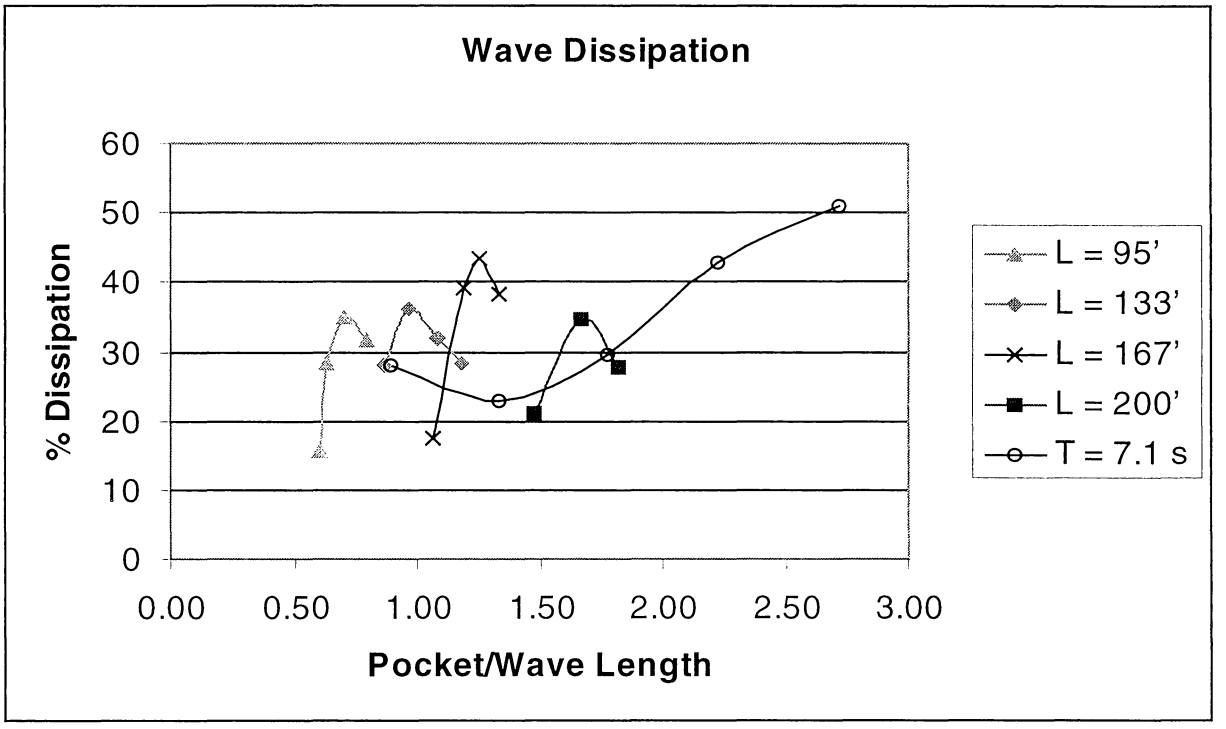

Figure 10: Percent wave energy dissipation versus pocket to wavelength ratios for four fixed pocket cases and the one fixed frequency case.

5.4 Pocket Location

A single 133-ft long pocket was placed in three different locations within the channel to determine if channel location was important for perpendicular incident waves (0-degree angle). The initial pocket location was 300 ft from the final wave gauge (see Figure 1), the second was 500 ft, and the third was 700 ft from the final wave gauge. As was expected for this case, the dissipation was not found to vary significantly with the dissipated amplitudes all being about the same (from .0268 to .0276). Appendix A shows that dissipation rate increased for the third case but that was attributed to the close proximity of the pocket to the initial wave gauge.

5.5 Angled Waves

To evaluate the effect of angled waves on pocket effectiveness, the incident wave propagation was directed at an angle of 30-degrees from the channel axis. A series of tests were then performed and compared to their 0-degree counterparts. The base conditions of stone size (2.1 ton), slope (1:2), pocket depth (40 ft), and frequency (1 Hz) were all maintained. A summary of the dissipation rates for most of the tests can be

found in Table 1. The headers in the table note the numbers of pockets as well as their length and location. Whenever two pockets were evaluated, they were placed on opposite sides of the channel. The offset case is when the two pockets, one on either side, were staggered so that the end of the first pocket was even with the beginning of the second.

Overall, it is easy to see that there is significantly more dissipation for every angled case considered. However, the amount of dissipation is a bit misleading because of the evaluation of the dissipated waves in the angled wave cases. To make comparisons between the two incident wave directions, they were both evaluated at the same wave gauge locations shown in Figure 1. These wave gauges yield very representative downstream wave amplitudes for the 0-degree tests, but the same thing cannot be said of the downstream wave amplitudes for the 30-degree case. The angled waves caused areas of constructive and destructive waves in the channel thereby affecting the wave amplitude. One example of this can be seen in the no pocket angled wave case. According to the probe, waves were dissipated by 39 percent. In truth, the overall dissipation rate was probably much less but the wave height at the probe location was smaller than in other nearby locations due to destructive interference. To examine this effect, the downstream wave gauge was moved one foot in the model in both the upstream and downstream directions to evaluate the effect on dissipated wave amplitudes. In some extreme cases the dissipated wave amplitudes changed by as much as 40 percent, which in turn would effect the dissipation rates by roughly 10 or 15 percent. This large of difference represents extreme cases and, in general, it can still be concluded that the angled waves were dissipated more than their 0-degree counterparts.

Table 1 also can be used to examine some potential pocket design considerations. For example, if two pockets are used they were more effective directly opposite each other instead of offset. Also, when considering both straight and angled waves, one 400-ft pocket was more effective than two 200-ft pockets. In addition, it was determined that little was gained by adding a second pocket. However, it should be noted that these

results only represent a singular frequency, a variable which was determined to play a significant role in wave energy dissipation.

	1 Pocket, L = 200'	Opposite Side, L = 200'	2 Pockets, L = 200'
Angled	66.7	68.8	60.5
Straight	22.8	22.8	30.0
	No Pocket	1 Pocket, L = 400'	Offset Pockets, L = 200'
Angled	39.0	58.7	48.1
Straight	10.3	50.9	12.0

Table 1: Percent dissipation for angled wave test comparisons.

6.0 ERROR ANALYSIS

All experimental measurements are subject to some uncertainty. The following is a list of potential error for the project:

- Water depth was kept primarily constant but slight variations in water depth over the course of the investigation can have an effect on the results. Overall this would be more of a problem in harbors with significant resonant interactions, but since the pocket length appears to have a resonant frequency, it could have some minor effects. For this investigation water depth was never allowed to vary by more than 5 percent.
- Wave reflections from the wave tank walls and the wave generator were limited by placing energy dissipation devices along the tank boundaries. This limited reflected energy but it is impossible to eliminate all reflections. This effect was further minimized by running tests for only 40 seconds after a 20 second start up time. This allowed the wave spectrum to be fully developed at all three wave gauges but limited the effect of tank reflections, which increase with time. The overall effect on wave amplitude uncertainty would be relatively small.
- The individual trials (labeled by configuration numbers) summarized in Appendix A represent the average of between 4 and 10 separate runs. The number of repetitions was dictated by repeatability. For example, if the amplitudes of the first four runs

differed by no more than 0.001 ft, then the trial was halted. If greater variability existed, than additional runs were made. Some specific examples can be found in Appendix B. It can be seen from these results that for a given trial the typical range is 0.002 with a standard deviation of 0.0008. This leads to uncertainties in the amplitudes on the order of less than 5 percent. The mean water levels (MWL) were also recorded for each run. This was done to insure that the capacitance probes were clean and recording properly. Significant variation in water levels (more than 0.003 ft) meant that the probes were not recording accurately (not clean) and the run was discounted.

- To make comparisons easier and results more meaningful, an attempt was made to keep the incident wave amplitudes equal for a given test. This was not always possible due to frequency changes, water depth variation, and tank reflections. A majority of the time, when making direct comparisons, the incident wave amplitudes did not vary by more than 5 percent. However, during the duration of the experiment care was not taken to ensure that the wave amplitudes were consistent. This was because during the early tests, the incident waves were set just below breaking and not to a set wave height. It was later determined that the incident wave height might play a role in energy dissipation. For example, configuration numbers 242a and 242b had dissipation rates of 62.8 percent and 50.9 percent respectively, with the only known difference being that their incident amplitudes differed, .0435 ft compared to .0393 ft. Conversely, configurations 342a and 342b had almost identical dissipation rates, 28.1 percent and 28.2 percent respectively, despite different incident wave amplitudes. Overall, the effect of incident wave height on dissipation was not determined.

7.0 CONCLUSIONS

The most important conclusion from this study is the effect resonance appears to have on wave energy dissipation. The general observed trend was that increased pocket length led to increased dissipation, but the relationship was not directly proportional. When evaluating the ratio of pocket length to wavelength, the complex relationship becomes

more evident, with maximum dissipation actually occurring at some intermediate frequency. This was apparently due to resonant interactions. Resonance occurs when a wave frequency approaches the natural frequency of an enclosed or partially enclosed area, such as the pocket. When this happens, wave motions can be amplified. The amplification of wave motion inside the pocket means that more wave energy interacts with the stone, thereby affecting observed dissipation. In addition, it appears as if incident wave heights might also affect dissipation, possibly in part since wave height affects wavelength in non-linear waves. This would then affect the specific period at which resonance occurs. Overall, an understanding of the relationship between resonance and wave energy dissipation was not fully determined but appears to play a significant role.

Other evaluated parameters yielded more defined results. For instance it was determined that slope of stone or pocket location within the channel had no significant effect. It was also determined that uniform stone size had no significant effect but that well sorted stone might. Therefore, void space of the placed stone might play a role, with reduced void space yielding lower dissipation rates. While this role was not fully determined, it probably is not relevant since pocket designs call for layers of uniform stone, not well sorted stone.

An attempt was made to evaluate how angled waves influence the effectiveness of the pockets. It was hard to evaluate the exact amount of wave energy dissipation for the angled wave cases. This was because only one downstream wave gauge was used and it was unable to capture the complex nature of the reflected waves for these cases. When angled waves enter the jetties, they reflect off of the walls creating regions of constructive and destructive interference. The downstream wave gauge might be located in one or the other of these regions. However, even though exact amounts of wave energy dissipation are hard to evaluate, it was shown that the straight incident wave cases represent the overall worst case scenarios.

8.0 RECOMMENDATIONS FOR FUTURE WORK

A better understanding of the relationship resonance has on wave energy dissipation is needed. Therefore it is recommended that this portion of the study be continued. A closer examination of the effect incident wave frequency and height has on wave dissipation would be performed with two methodologies.

First, we would fix pocket sizes and wave heights and make small incremental changes in the frequency to capture the entire range of pocket response to the incident wave conditions. This would allow us to better define the relationship between pocket length and the true wavelength.

Second, some cases would be repeated with different wave heights to determine the effect wave height plays on energy dissipation. This would allow us to determine if the role wave height plays is simply related because of the effect it has on nonlinear wavelengths or if the influence is less direct.

In addition, the effect of angled waves on energy dissipation was not fully quantified. Results were fairly conclusive that 0-degree incident waves represented "worst case" scenarios, but the exact amounts of dissipation were suspect because only one downstream wave gauge was used. Further tests should be run using an array of wave gauges downstream to better capture both constructive and destructive wave interference regions that result from wave reflections.

Finally, the depth of the pocket was never an evaluated variable. Because of the possibility of resonant interaction, pocket depth may also play an important role in energy dissipation. A series of tests could be performed to determine the influence pocket depth or overall pocket area has on energy dissipation.

APPENDIX A

Frequency – peak frequency of the test (Pg. 8)

Amplitude 1 – wave amplitude of the incident wave probe (Pg. 8)

Amplitude 2 – wave amplitude of the pocket wave probe (Pg. 8)

Amplitude 3 – wave amplitude of the dissipated wave probe (Pg. 8)

% Dissipation – [(amplitude 1 – amplitude 3) / amplitude 1] * 100 (Pg. 9)

Test: Slope

Configuration #	Frequency	Amplitude 1	Amplitude 2	Amplitude 3	% Dissipation	Notes
222	1.00	0.0393	0.0391	0.0193	50.89	1:2, 1 ton graded, L = 400’
221	1.00	0.0400	0.0354	0.0194	51.50	1:1.5, 1 ton graded, L = 400’
223	1.00	0.0402	0.0460	0.0185	53.98	1:3, 1 ton graded, L = 400’
341	1.00	0.0369	0.0390	0.0280	24.12	1:1.5, 2.1 ton uniform, L = 133’
343	1.00	0.0374	0.0406	0.0286	23.53	1:2, 2.1 ton uniform, L = 133’
342	1.00	0.0384	0.0426	0.0276	28.13	1:3, 2.1 ton uniform, L = 133’

Test: Stone Size

Configuration #	Frequency	Amplitude 1	Amplitude 2	Amplitude 3	% Dissipation	Notes
212	1.00	0.0421	0.0340	0.0179	57.48	.25 ton
222	1.00	0.0393	0.0391	0.0193	50.89	1 ton graded
232	1.00	0.0433	0.0399	0.0159	63.28	9 ton
242a	1.00	0.0435	0.0392	0.0162	62.76	2.1 ton
252	1.00	0.0443	0.0388	0.0172	61.17	.8 ton
262	1.00	0.0453	0.0388	0.0163	64.02	9 ton/.25 ton mix

Test: Location

Configuration #	Frequency	Amplitude 1	Amplitude 2	Amplitude 3	% Dissipation	Notes
342a	1.00	0.0384	0.0426	0.0276	28.13	Rear
642	1.00	0.0376	0.0432	0.0268	28.72	Middle
742	1.00	0.0415	0.0215	0.0275	33.73	Forward

Test: Length

Configuration #	Frequency	Amplitude 1	Amplitude 2	Amplitude 3	% Dissipation	Notes
342a	1.00	0.0384	0.0426	0.0276	28.13	L = 133’
142	1.00	0.0408	0.0347	0.0315	22.79	L = 200’
442	1.00	0.0378	0.0448	0.0266	29.63	L = 267’
542	1.00	0.0370	0.0432	0.0212	42.70	L = 333’
242b	1.00	0.0393	0.0391	0.0193	50.89	L = 400’

Test: Pocket/Wave Length

Configuration #	Frequency	Amplitude 1	Amplitude 2	Amplitude 3	% Dissipation	Notes
142	1.30	0.0354	0.0414	0.0256	27.68	L = 200’
142	1.20	0.0362	0.0388	0.0236	34.81	L = 200’
142	1.10	0.0350	0.0356	0.0276	21.14	L = 200’
142	1.00	0.0408	0.0347	0.0315	22.79	L = 200’
142	0.90	0.0350	0.0354	0.0320	8.57	L = 200’
342	1.30	0.0346	0.0412	0.0248	28.32	L = 133’
342	1.20	0.0360	0.0395	0.0245	31.94	L = 133’
342	1.10	0.0386	0.0388	0.0246	36.27	L = 133’
342	1.00	0.0384	0.0426	0.0276	28.13	L = 133’
342	0.90	0.0376	0.0434	0.0372	1.06	L = 133’
842	1.20	0.0380	0.0350	0.0260	31.58	L = 95’
842	1.10	0.0370	0.0340	0.0240	35.14	L = 95’
842	1.00	0.0378	0.0383	0.0271	28.31	L = 95’
842	0.95	0.0380	0.0380	0.0320	15.79	L = 95’
942	1.20	0.0380	0.0380	0.0235	38.16	L = 167’
942	1.15	0.0388	0.0360	0.0220	43.30	L = 167’
942	1.10	0.0378	0.0370	0.0230	39.15	L = 167’
942	1.00	0.0366	0.0398	0.0302	17.49	L = 167’

Test: Two Pockets - Straight and Angled Waves

Configuration #	Frequency	Amplitude 1	Amplitude 2	Amplitude 3	% Dissipation	Notes
1042	1.00	0.0400	0.0320	0.0280	30.00	L = 200’ straight
1142	1.00	0.0390	0.0450	0.0380	2.56	L = 133’ straight
1242a	1.00	0.0410	0.0370	0.0100	75.61	L = 133’ angled
1342	1.00	0.0400	0.0388	0.0158	60.50	L = 200’ straight
1742	1.00	0.0412	0.0142	0.0214	48.06	L = 200’ angled offset
1942	1.00	0.0375	0.0310	0.0330	12.00	L = 200’ straight offset

Test: Angled Waves

Configuration #	Frequency	Amplitude 1	Amplitude 2	Amplitude 3	% Dissipation	Notes
1542a	1.00	0.0418	0.0393	0.0255	39.00	No Pocket
1642	1.00	0.0404	0.0398	0.0126	68.81	L = 200' (opp. conf 1)
1442	1.00	0.0408	0.0410	0.0136	66.67	L = 200' (conf 1)
1842	1.00	0.0392	0.0128	0.0162	58.67	L = 400' (conf 2)

Test: Channel Width

Configuration #	Frequency	Amplitude 1	Amplitude 2	Amplitude 3	% Dissipation	Notes
2142	1.00	0.0340	0.0440	0.0245	27.94	W = 150'
142	1.00	0.0408	0.0347	0.0315	22.79	W = 200'
2242	1.00	0.0340	0.0380	0.0150	55.88	W = 250'

Test: Other Runs

Configuration #	Frequency	Amplitude 1	Amplitude 2	Amplitude 3	% Dissipation	Notes
122	1.00	0.0400	0.0450	0.0330	17.50	
222	1.20	0.0508	0.0427	0.0242	52.36	
222	0.90	0.0407	0.0340	0.0255	37.35	
342b	1.00	0.0415	0.0385	0.0298	28.19	
1242b	1.00	0.0408	0.0395	0.0138	66.18	Rear Probe 1' forward
1542b	1.00	0.0405	0.0403	0.0430	-6.17	Rear Probe 1' forward
2042	1.00	0.0380	0.0370	0.0325	14.47	200' stone in channel
Plain Channel	1.00	0.0390	0.0360	0.0350	10.26	

Configuration Number Explanation:

The first number stands for the jetty configuration, the second stands for stone size, and the third for slope.
If two configurations were tested using the same frequency, they are designated with a letter following the number.

Stone Size	Number	Slope	Number
.25 ton	1	1:1.5	1
1 ton graded	2	1:2	2
9 ton	3	1:3	3
2.1 ton	4		
.8 ton	5		
.25 & 9 ton mix	6		

APPENDIX B

Configuration 1842

Run	Amplitude 1	Amplitude 3	MWL 1	MWL 2	Freq.
a	0.039	0.015	0.325	0.347	1.00
b	0.038	0.015	0.325	0.347	1.00
c	0.040	0.017	0.325	0.347	1.00
d	0.039	0.017	0.325	0.347	1.00
e	0.040	0.017	0.325	0.347	1.00
f	0.039	0.016	0.325	0.347	1.00
Average	**0.0392**	**0.0162**	**0.3250**	**0.3470**	
Range	**0.020**	**0.020**	**0.000**	**0.000**	
Std Dev	**0.0007**	**0.0009**	**0.0000**	**0.0000**	

Configuration 142

Run	Amplitude 1	Amplitude 3	MWL 1	MWL 2	Freq.
a	0.035	0.032	0.319	0.341	0.09
b	0.035	0.031	0.320	0.341	0.09
c	0.035	0.033	0.319	0.341	0.09
d	0.035	0.033	0.321	0.341	0.09
e	0.035	0.032	0.319	0.341	0.09
Average	**0.0350**	**0.0322**	**0.3196**	**0.3410**	
Range	**0.000**	**0.020**	**0.020**	**0.000**	
Std Dev	**0.0000**	**0.0007**	**0.0008**	**0.0000**	

Configuration 212

Run	Amplitude 1	Amplitude 3	MWL 1	MWL 2	Freq.
a	0.041	0.016	0.319	0.34	1.00
b	0.041	0.018	0.319	0.341	1.00
c	0.042	0.018	0.319	0.341	1.00
d	0.042	0.018	0.319	0.341	1.00
e	0.044	0.020	0.321	0.341	1.01
f	0.043	0.018	0.320	0.341	1.01
g	0.042	0.018	0.318	0.341	1.01
h	0.042	0.017	0.319	0.34	1.01
Average	**0.0421**	**0.0179**	**0.3193**	**0.3408**	
Range	**0.020**	**0.020**	**0.020**	**0.020**	
Std Dev	**0.0009**	**0.0011**	**0.0008**	**0.0004**	

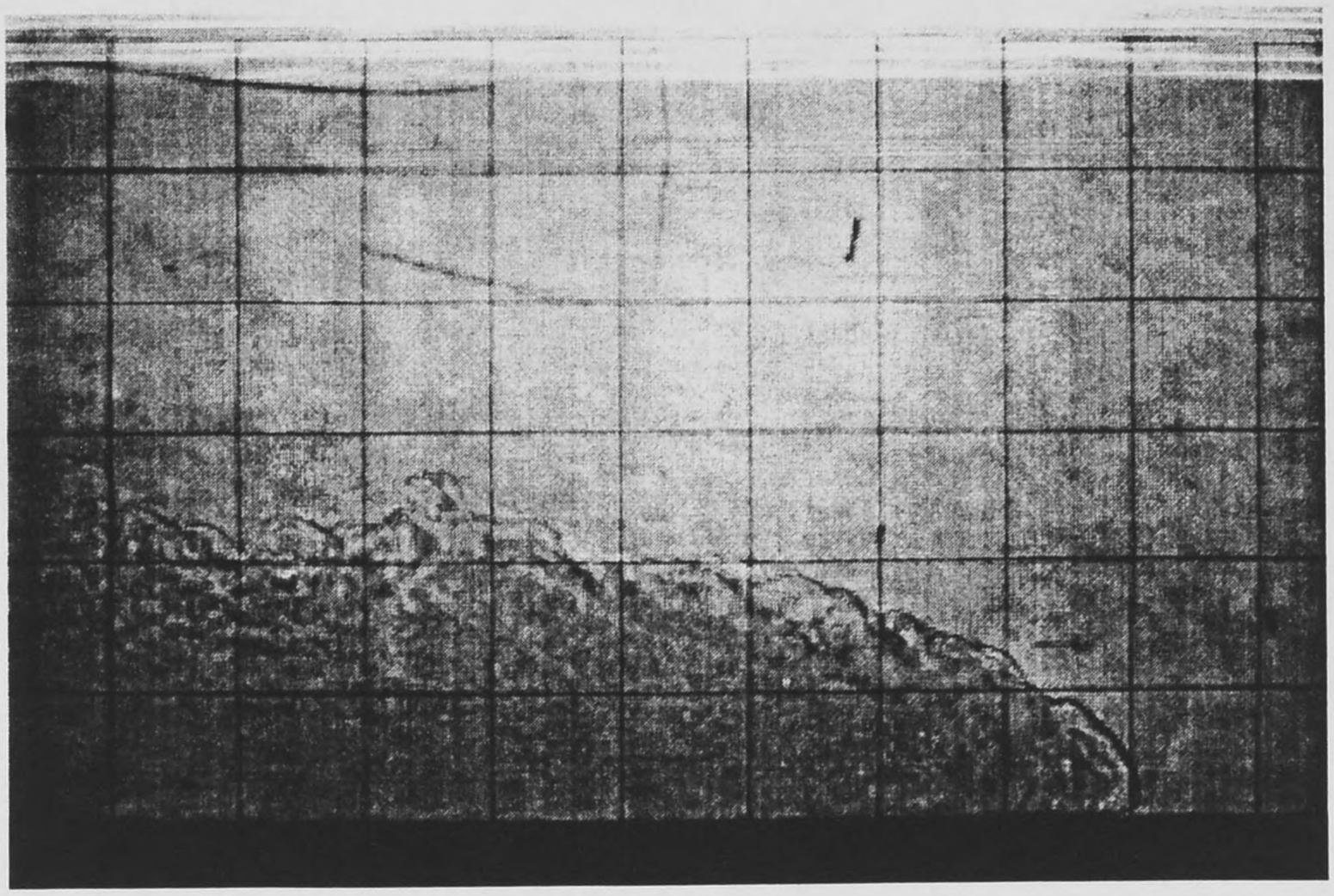

Figure 5.2 Density Current in Lock Exchange Conditions.

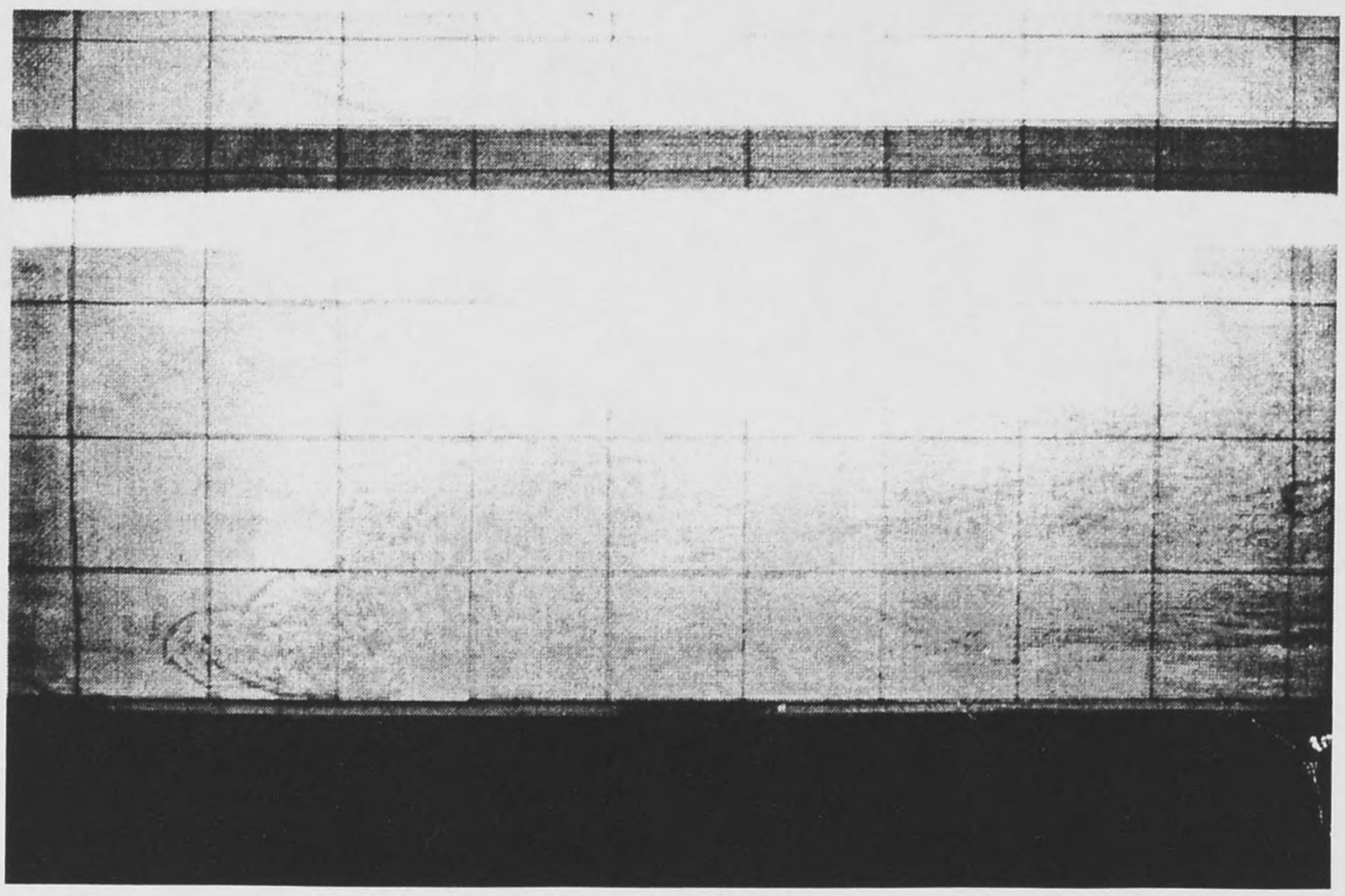

Figure 5.3 Density Current in Coflow Conditions.

AIIM SCANNER TEST CHART # 2

Spectra

4 PT ABCDEFGHIJKLMNOPQRSTUVWXYZabcdefghijklmnopqrstuvwxyz:'',./?$0123456789

6 PT ABCDEFGHIJKLMNOPQRSTUVWXYZabcdefghijklmnopqrstuvwxyz;:'',./?$0123456789

8 PT ABCDEFGHIJKLMNOPQRSTUVWXYZabcdefghijklmnopqrstuvwxyz;:'',./?$0123456789

10 PT ABCDEFGHIJKLMNOPQRSTUVWXYZabcdefghijklmnopqrstuvwxyz;:'',./?$0123456789

Times Roman

4 PT ABCDEFGHIJKLMNOPQRSTUVWXYZabcdefghijklmnopqrstuvwxyz;:'',./?$0123456789

6 PT ABCDEFGHIJKLMNOPQRSTUVWXYZabcdefghijklmnopqrstuvwxyz;:'',./?$0123456789

8 PT ABCDEFGHIJKLMNOPQRSTUVWXYZabcdefghijklmnopqrstuvwxyz;:'',./?$0123456789

10 PT ABCDEFGHIJKLMNOPQRSTUVWXYZabcdefghijklmnopqrstuvwxyz;:'',./?$0123456789

Century Schoolbook Bold

4 PT **ABCDEFGHIJKLMNOPQRSTUVWXYZabcdefghijklmnopqrstuvwxyz;:'',./?$0123456789**

6 PT **ABCDEFGHIJKLMNOPQRSTUVWXYZabcdefghijklmnopqrstuvwxyz;:'',./?$0123456789**

8 PT **ABCDEFGHIJKLMNOPQRSTUVWXYZabcdefghijklmnopqrstuvwxyz;:'',./?$0123456789**

10 PT **ABCDEFGHIJKLMNOPQRSTUVWXYZabcdefghijklmnopqrstuvwxyz;:'',./?$0123456789**

News Gothic Bold Reversed

4 PT ABCDEFGHIJKLMNOPQRSTUVWXYZabcdefghijklmnopqrstuvwxyz;:'',./?$0123456789

6 PT ABCDEFGHIJKLMNOPQRSTUVWXYZabcdefghijklmnopqrstuvwxyz;:'',./?$0123456789

8 PT ABCDEFGHIJKLMNOPQRSTUVWXYZabcdefghijklmnopqrstuvwxyz;:'',./?$0123456789

10 PT ABCDEFGHIJKLMNOPQRSTUVWXYZabcdefghijklmnopqrstuvwxyz;:'',./?$0123456789

Bodoni Italic

4 PT ABCDEFGHIJKLMNOPQRSTUVWXYZabcdefghijklmnopqrstuvwxyz;:'',./?$0123456789

6 PT ABCDEFGHIJKLMNOPQRSTUVWXYZabcdefghijklmnopqrstuvwxyz;:'',./?$0123456789

8 PT ABCDEFGHIJKLMNOPQRSTUVWXYZabcdefghijklmnopqrstuvwxyz;:'',./?$0123456789

10 PT ABCDEFGHIJKLMNOPQRSTUVWXYZabcdefghijklmnopqrstuvwxyz;:'',./?$0123456789

Greek and Math Symbols

4 PT ΑΒΓΔΕΞΘΗΙΚΛΜΝΟΠΦΡΣΤΥΩΧΨΖαβγδεξθηικλμνοπφρστυωχψζ≧∓'',. / ≦±=≠°><⊁⊀⩾⩽≡

6 PT ΑΒΓΔΕΞΘΗΙΚΛΜΝΟΠΦΡΣΤΥΩΧΨΖαβγδεξθηικλμνοπφρστυωχψζ≧∓'',. / ≦±=≠°><⊁⊀⩾⩽≡

8 PT ΑΒΓΔΕΞΘΗΙΚΛΜΝΟΠΦΡΣΤΥΩΧΨΖαβγδεξθηικλμνοπφρστυωχψζ≧∓'',. / ≦±=≠°><⊁⊀⩾⩽≡

10 PT ΑΒΓΔΕΞΘΗΙΚΛΜΝΟΠΦΡΣΤΥΩΧΨΖαβγδεξθηικλμνοπφρστυωχψζ≧∓'',. / ≦±=≠°><⊁⊀⩾⩽≡

White

Black

Isolated Characters

e	m	1	2	3	a
4	5	6	7	o	°
8	9	0	h	I	B

A4 Page 6543210

MESH HALFTONE WEDGES

65

85

100

110

133

150

A4 Page 6543210

RIT ALPHANUMERIC RESOLUTION TEST OBJECT, RT-1-71

PRODUCED BY GRAPHIC ARTS RESEARCH CENTER

ROCHESTER INSTITUTE OF TECHNOLOGY, ONE LOMB

MEMORIAL DRIVE, ROCHESTER, NEW YORK 14623